Eur. Phys. J. A **22**, 179–188 (2004)
DOI 10.1140/epja/i2004-10041-9

THE EUROPEAN PHYSICAL JOURNAL A

Description of ^{111}Ru within the Core-Quasiparticle Coupling model

Ch. Droste[1], S.G. Rohoziński[1,a], L. Próchniak[2], K. Zając[2], W. Urban[1], J. Srebrny[1], and T. Morek[1]

[1] Faculty of Physics, Warsaw University, ul. Hoża 69, PL-00-681 Warsaw, Poland
[2] Institute of Physics, Maria Curie-Skłodowska University, Pl. M. Curie-Skłodowskiej 1, PL-20-031 Lublin, Poland

Received: 1 April 2004 /
Published online: 9 November 2004 –
Communicated by G. Orlandini

Abstract. An even-odd isotope of ruthenium, ^{111}Ru, is investigated in the framework of the Core-Quasiparticle Coupling model. The energy levels and wave functions of low-lying states are calculated. The only one parameter adjusted to obtain the results in agreement with experimental data is the strength of the core-particle quadrupole-quadrupole interaction. The neighbouring even-even cores, ^{110}Ru and ^{112}Ru, are described by means of the collective "quadrupole plus pairing" model with the Bohr Hamiltonian determined fully from a microscopic theory without any adjustable parameter. Results for ^{111}Ru are compared with a new set of experimental data obtained recently. An importance of the pairing interaction is confirmed. A remarkable agreement of theoretical results and experimental data is obtained for all eight positive- and negative-parity bands delivered by the newest experiment.

PACS. 21.10.Re Collective levels – 21.60.Ev Collective models – 23.20.Lv γ transitions and level energies – 27.60.+j $90 \leq A \leq 149$

1 Introduction

New comprehensive experimental data for nuclei of the $A \approx 110$ region became available in the last decade. The spontaneous fission process is often utilized to produce nuclei of that mass region. Spectroscopic properties of fission products are investigated by means of prompt gamma spectroscopy using multi-detector arrays. Collective states of the even-even isotopes $^{108-114}$Ru have already been observed some time ago [1]. Recently, the prompt gamma spectroscopy of fission products of ^{248}Cm was used to obtain a new set of data for even-odd nucleus ^{111}Ru [2]. It is now a challenge to theoretical models to describe and explain the structure of this nucleus.

Odd-A nuclei have for years been described by means of the Core-Quasiparticle Coupling (CQPC) model [3–5]. The separable quadrupole-quadrupole interaction between the even-even core and odd nucleon causes that, apart from the core excitation energies, the quadrupole matrix elements within the core states appear in calculations of the odd-nucleus structure. Experimental data for all these characteristics of even-even nuclei have, as a rule, been too scarce to form a basis for such calculations. This is why the core data have usually been taken from a theory. The even-even isotopes, ^{110}Ru and ^{112}Ru, neighbouring to ^{111}Ru, have been described theoretically in the frame of a phenomenological General Collective Model in ref. [6]. That approach demands, however, adjusting a few free parameters to reproduce the experimental data. A few years ago the "quadrupole plus pairing" collective model has been developed for description of low-lying collective states of even-even nuclei (cf. [7,8]). The model has allowed us to describe in a satisfactory way these even-even Ru isotopes without any adjustable parameters starting from a microscopic many-body Hamiltonian [7]. What is more, that collective approach to even-even nuclei suggests a natural extension of the CQPC model to odd-A systems [8].

The aim of the present research is just the description of the low-energy structure of ^{111}Ru in the frame of the CQPC model. We are going to use for the first time the core data calculated from a microscopic many-body theory through the "quadrupole plus pairing" collective model. We intend to confront the results of calculation with the newest experimental data for the ^{111}Ru nucleus [2]. To this end, we first recapitulate briefly the CQPC model and the method of description of the cores in sect. 2 and sect. 3, respectively. Application of the models mentioned above to the problem of ^{111}Ru is presented in sect. 4. Section 4.1 handles the input data to be used in the calculation. The characteristics of the ^{110}Ru and ^{112}Ru cores, the single-particle basis of the neutron states and the strength of core-particle quadrupole-quadrupole coupling are discussed in turn in sects. 4.1.1, 4.1.2 and 4.1.3. Section 4.2

[a] e-mail: Stanislaw-G.Rohozinski@fuw.edu.pl

is devoted to a presentation and discussion of the results which are compared with the experimental data. Finally, in sect. 5 we sum up the results and draw conclusions from the present research.

2 Outline of the Core-Quasiparticle Coupling model

The microscopic ground for the Core-Quasiparticle Coupling (CQPC) model [3–5] are the equations of motion with the schematic "quadrupole plus pairing" many-body Hamiltonian (cf. ref. [9]), which is supposed to render the most essential properties of the nucleon-nucleon interaction in nuclei:

$$H = H_{\rm sp} - \frac{1}{2}\chi_2 Q_2^\dagger \cdot Q_2 - \frac{1}{4}\sum_{t=n,p} G_t P_t^\dagger P_t \,. \qquad (1)$$

where the one-body operators $H_{\rm sp}$ and Q_2 are the single-particle mean-field Hamiltonian and the total mass quadrupole moment, respectively, the dot stands for scalar product and P_t is the transfer operator of pair of like nucleons of kind $t\,(=n,p)$ in single-particle states time-reversed to each other.

Let the states of the odd-A nucleus in question be denoted as $|JM,A\rangle$ and the states of the even-even cores of mass numbers $A-1$ and $A+1$ as $|RM_R,A-1\rangle$ and $|RM_R,A+1\rangle$, respectively, where J and R stand for the corresponding spins (and remaining quantum numbers). The single-particle states are to be labelled with j, their total angular momenta. The CQPC model is a linearization and approximation of the equations of motion for the amplitudes of single-particle and single-hole spectroscopic factors, $u_J(j,R)$ and $v_J(j,R)$, respectively. (cf. *e.g.* refs. [10,11]). The corresponding Hamiltonian matrix to diagonalize has the form

$$\begin{aligned}&\mathcal{H}_{\rm odd}(j,R;j',R') = \\ &= \begin{bmatrix}[E^{(-)}]+[h^{(-)}] & [D_t] \\ [D_t] & [E^{(+)}]-[h^{(+)}]\end{bmatrix}, \end{aligned} \qquad (2)$$

where index t defines the odd nucleon. The submatrices appearing in eq. (2) read

$$E^{(\mp)}(j,R;j',R') = E(R,A\mp 1)\delta_{RR'}\delta_{jj'}\,, \qquad (3)$$

$$\begin{aligned}&h^{(\mp)}(j,R;j',R') = (e_j-\lambda)\delta_{jj'}\delta_{RR'} \\ &-\frac{1}{2}\chi_2(-1)^{j'+R+J}\left\{\begin{matrix} j & j' & 2 \\ R' & R & J\end{matrix}\right\}\langle j||q_2||j'\rangle \\ &\times\langle R,A\mp 1||Q_2||R',A\mp 1\rangle, \end{aligned} \qquad (4)$$

$$\begin{aligned}&D_t(j,R;j',R') \\ &= G_t\langle RM_R,A-1|P_t|R'M'_R,A+1\rangle\delta_{jj'}\,, \end{aligned} \qquad (5)$$

where $E(R,A\mp 1)$ are the excitation energies of the cores, e_j are the single-particle energy levels of nucleon t, q_2 is the single-particle quadrupole operator and λ is the Fermi level. All quantities appearing in eqs. (3), (4) and (5) are considered as known. These constitute the input to the model. A subset of eigenvalues $\mathcal{E}_k(J,A)$ (k numbers the eigenvalues of the same J) of the matrix of eq. (2) gives the excitation energies of the odd-A nucleus. References [4,11] can be consulted in question how to choose the physical solutions and how to calculate all relevant matrix elements of observables within the odd-nucleus states.

Since the CQPC model is a linearized theory, the quantities, which occur in eqs. (3), (4) and (5), related to the cores are treated as given. These are: the energy levels $E(R,A\mp 1)$, the quadrupole reduced matrix elements $\langle R,A\mp 1||Q_2||R',A\mp 1\rangle$ and the pairing correlation energy matrix elements $D_t(j,R;j',R')$. Thus, the model does not, obviously, take into account the effect of core polarization induced by the odd particle. The effect can be simulated partially by changing the quadrupole interaction strength χ_2 what roughly means a change of the core deformation felt by the odd particle. Therefore, χ_2 is usually treated as a free parameter of the model.

3 Description of the cores

It is used to believe that the best way to get good results for odd nuclei is to take the experimental data for the cores and insert them into CQPC model. However, it is by far not obvious that this is really the best thing to do. Anyway, such a procedure is hardly realizable in practice since there is often a lack of comprehensive experimental data. Especially, the information about matrix elements $\langle R,A\mp 1||Q_2||R',A\mp 1\rangle$ is usually scarce. Therefore, a theoretical description of the even-even nuclei should be utilized instead.

The generalized collective "quadrupole plus pairing" Bohr Hamiltonian [8] is in the present paper applied to the description of the collective excitations of even-even nuclei. In this version of the Bohr Hamiltonian the moduli and phases of the ground-state mean values of the neutron and proton pairing correlation energies, *i.e.* the pairing energy gap parameters, Δ_n, Δ_p and the gauge angles, ϕ_n, ϕ_p, apart from the usual Bohr quadrupole deformation parameters, β and γ and the Euler angles, φ, ϑ, ψ, are used as the collective variables. Again, this is the microscopic many-body Hamiltonian of eq. (1) which prompts us to define that collective space. The model thus describes not only the lowest, quadrupole collective nuclear excitations but also the pairing vibrations coupled to them as well as the collective pair transfer between neighbouring even-even nuclei. The collective model Hamiltonian has the following structure:

$$\begin{aligned}&\mathcal{H}_{\rm even}(\beta,\gamma,\varphi,\vartheta,\psi,\Delta_n,\phi_n,\Delta_p,\phi_p) \\ &= \mathcal{T}_{\rm qv}(\partial/\partial\beta,\partial/\partial\gamma,\beta,\gamma,\Delta_n,\Delta_p) \\ &+\mathcal{T}_{\rm qr}(\mathbf{R}(\partial/\partial\varphi,\partial/\partial\vartheta,\partial/\partial\psi,\varphi,\vartheta,\psi),\beta,\gamma,\Delta_n,\Delta_p) \\ &+\mathcal{T}_{\rm pv}(\partial/\partial\Delta_n,\partial/\partial\Delta_p,\beta,\gamma,\Delta_n,\Delta_p) \\ &+\mathcal{T}_{\rm pr}(\partial/\partial\phi_n,\partial/\partial\phi_p,\beta,\gamma,\Delta_n,\Delta_p) \\ &+\mathcal{T}_{\rm qp}(\partial/\partial\beta,\partial/\partial\gamma,\partial/\partial\Delta_n,\partial/\partial\Delta_p,\beta,\gamma,\Delta_n,\Delta_p) \\ &+\mathcal{V}_{\rm def}(\beta,\gamma,\Delta_n,\Delta_p)+\mathcal{V}_{\rm pair}(\beta,\gamma,\Delta_n,\Delta_p), \end{aligned} \qquad (6)$$

where $\mathcal{T}$'s are the kinetic energy operators of the quadrupole vibrations, quadrupole rotations, pairing vibrations, pairing rotations (*i.e.* pair transfer), and mixed quadrupole and pairing vibrations, respectively, $\mathcal{V}$'s are deformation and pairing potentials, respectively, and $\mathbf{R}$ is the angular momentum operator being a differential operator in the Euler angles. The quadrupole excitations alone have been treated so far in the frame of a version of the Born-Oppenheimer approximation for the Hamiltonian of eq. (6) which reads

$$\begin{aligned}&\mathcal{H}_{\rm quad}(\beta,\gamma,\varphi,\vartheta,\psi)\\&=\mathcal{T}_{\rm qv}(\partial/\partial\beta,\partial/\partial\gamma,\beta,\gamma,\bar{\Delta}_n(\beta,\gamma),\bar{\Delta}_p(\beta,\gamma))\\&+\mathcal{T}_{\rm qr}(\mathbf{R}(\varphi,\vartheta,\psi),\beta,\gamma,\bar{\Delta}_n(\beta,\gamma),\bar{\Delta}_p(\beta,\gamma))\\&+\mathcal{V}_{\rm def}(\beta,\gamma,\bar{\Delta}_n(\beta,\gamma),\bar{\Delta}_p(\beta,\gamma))+E_{\rm pair}(\beta,\gamma)\end{aligned}\tag{7}$$

where $\bar{\Delta}_n$ and $\bar{\Delta}_p$ are the most probable values of the neutron and proton pairing energy gap parameters in the zero-point pairing vibration state of energy $E_{\rm pair}$ for given values of β and γ. This state is the ground state of the pairing Hamiltonian

$$\mathcal{H}_{\rm pair}=\mathcal{T}_{\rm pv}+\mathcal{V}_{\rm pair}\tag{8}$$

for arbitrary values of β and γ. More information concerning details of the model is given *e.g.* in refs. [7,8]. The effect of zero-point pairing vibration on the quadrupole excitations is essential. When taken into account this effect improves description of the collective excitations very much. That way we have obtained for the first time results compatible with experimental data using the collective Hamiltonian calculated from a microscopic theory without any free parameters. Solution of the Hamiltonian of eq. (7) yields the quantities which are an input to the CQPC model: excitation energies $E_k(R,A\mp1)$ of collective states R_k^+ of both cores (k numbers the solutions of given R and superscript "+" stands for positive parity), collective wave functions and in consequence the quadrupole reduced matrix elements $\langle R,A\mp1||Q_2||R',A\mp1\rangle$. However, the Born-Oppenheimer approximation applied to the description of the quadrupole excitations alone does not allow us to calculate the pair transfer matrix elements $D_t(j,R;j',R')$ from the model. This would be possible only when solving the model exactly and describing at the same time both, the pairing vibrations and the rotations or the pair transfer. The matrix elements calculated this way would be obviously treated as given input quantities in the CQPC model. Thus, a kind of polarization effect by the odd nucleon, usually understood as the blocking effect, would not be taken into account. It could be tried to consider partially by a renormalization of the pairing interaction strength G_t.

4 The CQPC calculations for ^{111}Ru

Properties of nuclide $^{111}_{44}$Ru$_{67}$ are described here in the framework of the CQPC model discussed in sect. 2. In the present case, the odd particle is the neutron ($t=n$) and the cores are $^{110}_{44}$Ru$_{66}$ and $^{112}_{44}$Ru$_{68}$.

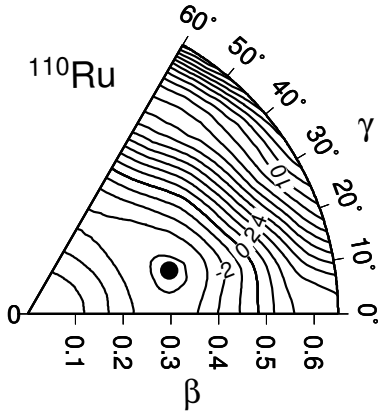

Fig. 1. Map of the calculated collective potential energy surface for ^{110}Ru. Deformations β and γ are the polar coordinates on the plane. Contour lines are every 1 MeV. The black circle points the minimum of the potential.

4.1 Input data

The input data to the present CQPC model calculations are presented in sects. 4.1.1, 4.1.2 and 4.1.3 below.

4.1.1 Characteristics of the cores

To simplify the calculations, the ^{110}Ru data have been taken for both, the $A-1$ and $A+1$ cores. Such a procedure is admissible because of a similarity of properties of both nuclei at low excitation energies. For instance, the excitation energies of the first 2^+ and 10^+ levels of ^{110}Ru are equal to 240 keV and 2758 keV, respectively, whereas the corresponding values for ^{112}Ru are 236 keV and 2563 keV [1]. Also, the value of $B(E2;2^+\to0^+)\approx0.22\,e^2b^2$ is the same for both nuclei within the experimental error [12]. The excitation energies and the quadrupole matrix elements of ^{110}Ru are taken from ref. [7] where the collective model calculations are presented for ruthenium isotopes. The collective Hamiltonian of sect. 3 has been determined in an entirely microscopic way there. According to the calculation ^{110}Ru is a γ-soft triaxial nucleus. The calculated ground-state mean values of deformations β and γ are equal to $\langle\beta\rangle=0.30$ and $\langle\gamma\rangle=21°$, respectively. The corresponding dispersions of deformations in the ground state are $\sigma(\beta)=0.06$ and $\sigma(\gamma)=10°$. Let us recall ourselves in this place that the maximum value of $\sigma(\gamma)$ is about 11°. The calculated potential energy surface is shown in fig. 1. The theoretical level scheme of ^{110}Ru is compared with the experimental data [13] in fig. 2. One can see that the model reproduces the experimental data quite well in spite of the calculation has been performed without fitting any parameter.

As many as 35 core states up to spin $R=16$ have been included in the calculation. It turns out that only the core states of spins $R\le10$ contribute substantially to the wave functions of the ^{111}Ru states discussed here.

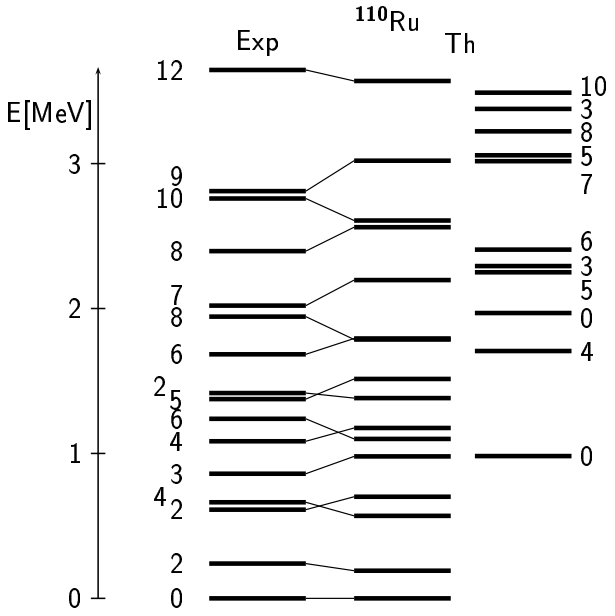

Fig. 2. Positive-parity levels $E_k(R, 110)$ of ^{110}Ru. Each level is marked with the spin value. The three lowest levels ($k = 1, 2, 3$) of a given spin are drawn. The levels calculated in ref. [7] which have their experimental counterparts [13] (left column) are placed in the middle column. Those calculated but not observed experimentally are drawn on the right part of figure.

Therefore, the basis of the collective states used in the calculations seems to be by far sufficient to reproduce the properties of the ^{111}Ru nucleus.

The state-independent pairing correlation energy matrix

$$D_n(j, R; j', R') = \Delta_n \delta_{jj'} \delta_{RR'}, \qquad \Delta_n = 135\,\mathrm{MeV}/A \tag{9}$$

is, according to the standard formula, taken to the calculations. The position of the Fermi level λ is chosen as to reproduce the number of valence neutrons in ^{111}Ru with this gap value (see fig. 3).

4.1.2 Basis of the single-neutron states

The basis of single-neutron states taken to the calculation contains all orbitals of the valence spherical shell $50 < N \leq 82$, namely: $2d_{5/2}$, $1g_{7/2}$, $3s_{1/2}$, $2d_{3/2}$ of the positive-parity and the negative-parity intruder $1h_{11/2}$. To reproduce the negative- and positive-parity states in ^{111}Ru the basis has to be supplemented by the negative-parity states $2f_{7/2}$, $2f_{5/2}$, $3p_{3/2}$, $3p_{1/2}$ from the upper shell and the positive-parity orbital $1g_{9/2}$ from the lower shell. Especially, the $3p_{3/2}$ and $3p_{1/2}$ negative-parity states strongly affect the positions of the low-lying, low-spin, negative-parity states of ^{111}Ru. On the other hand, the negative-parity state $1h_{9/2}$, the positive-parity intruder $1i_{13/2}$, both of the upper shell and all the negative-parity states of the lower $28 < N \leq 50$ shell are excluded from the basis as being of no importance in the calculation. The single-neutron energy spectrum in the vicinity of the Fermi level λ for ^{111}Ru is shown in fig. 3. To be in agreement with the core calculations, we used the same energies of the single-neutron states as used in ref. [7]. As the position of the Fermi level is in the middle of the valence shell, strong pairing effects are expected meaning that all single-particle states are of the quasiparticle character. Neither the effective nonzero charge nor the orbital g-factor for the valence neutron are used. The standard value of the effective spin g-factor, $g_s^{\mathrm{eff}} = 0.6 g_s^n$, is taken when calculating electromagnetic properties of the odd nucleus.

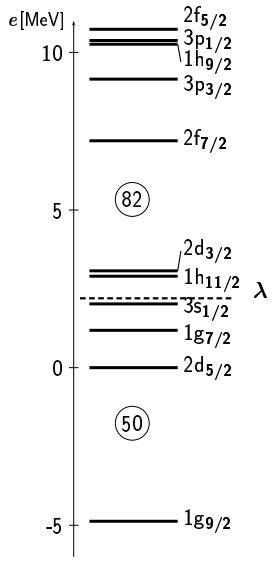

Fig. 3. Single-neutron states in the Nilsson spherical potential parameterized as in ref. [14]. The dashed line denotes the position of the Fermi level λ. The set of levels is very similar to that shown in ref. [15] for $A \approx 110$.

4.1.3 Strength of the core-particle quadrupole interaction

As is seen from eq. (4) the quadrupole-quadrupole coupling constant χ_2 plays the role of the strength of the quadrupole-quadrupole interaction between the valence neutron and each of the cores in the model. It is the only one fitted parameter in the present calculation. The reasonable agreement between calculated and experimental characteristics of ^{111}Ru for both, positive- and negative-parity states, has been obtained for $\chi_2 = 15\,\mathrm{MeV}$. A theoretical estimation done in ref. [9] gives a value $\chi_2 \approx 40\,\mathrm{MeV}$ for ^{111}Ru, whereas the value $\chi_2 \approx 11\,\mathrm{MeV}$ is suggested in ref. [16]. This latter value is quite close to that fitted in the present analysis. It is worth mentioning that in the CQPC calculations performed for ^{111}Te [17] of the same mass number as that considered here, a good agreement between the theoretical and experimental energies of the $15/2^-$, $17/2^-$ and $19/2^-$ levels belonging to the $\nu h_{11/2}$ decoupled band has been obtained for values of χ_2 in the range 9–14 MeV. This result is also in favour of the estimation of ref. [16] rather than that of ref. [9].

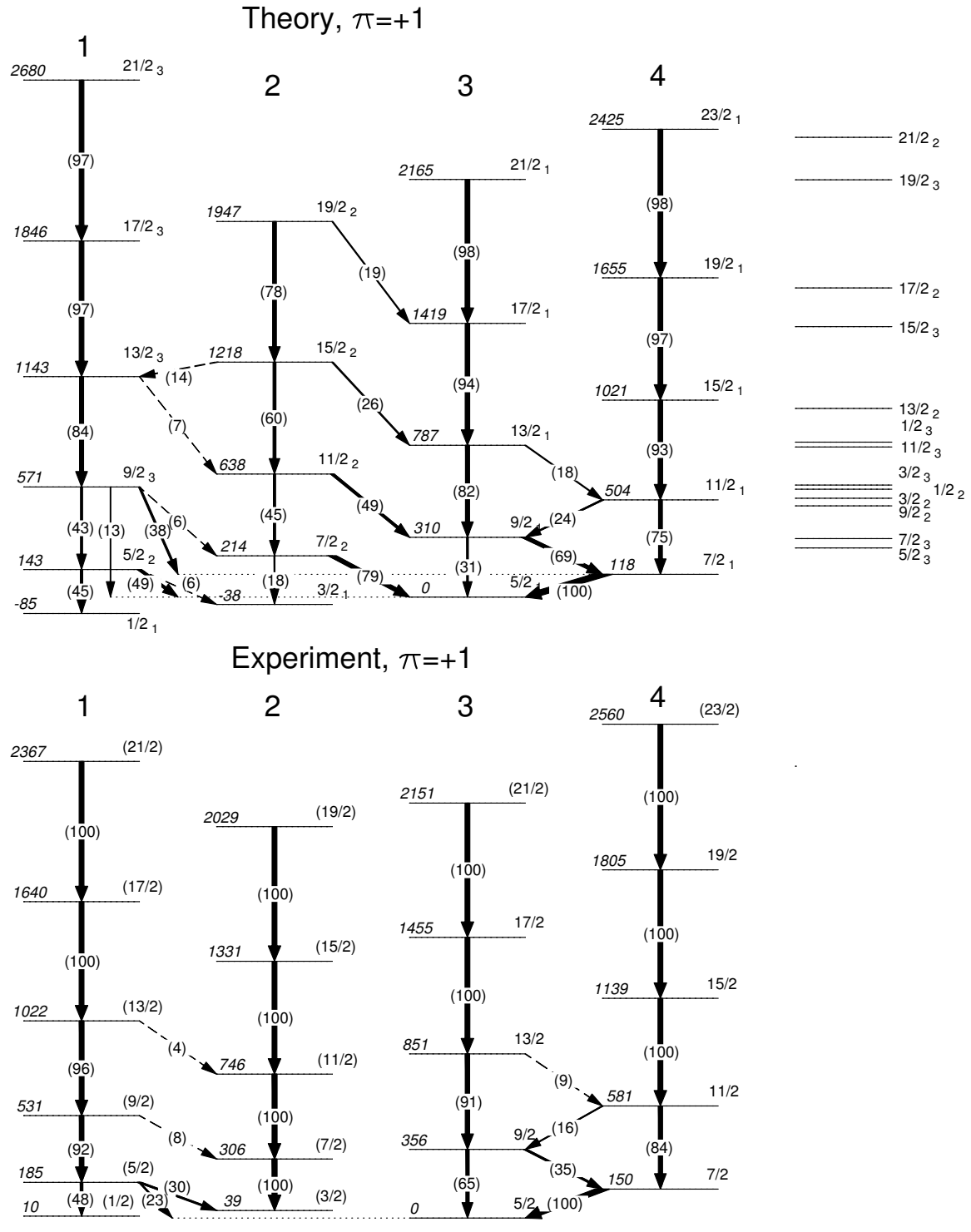

Fig. 4. Positive-parity states in ^{111}Ru. Top: the results of the present CQPC model calculations. The three lowest states of a given spin are drawn. Those states which have not their counterparts in the experiment are grouped in the rightmost column. Numbering of the bands is arbitrary. The energy of the first $5/2^+$ state is normalized to zero. The width of arrows is proportional to the γ-transition intensity. The sum of intensities of all γ-transitions leaving the given state is assumed to be 100. Bottom: a part of the experimental level scheme of ref. [2].

4.2 The results

One quasi-particle positive- and negative-parity states of ^{111}Ru are calculated in the frame of the CQPC model using the input data discussed in sect. 4.1 above. The present research gives up to the six lowest ($k = 1, \ldots, 6$) excitation energies $\mathcal{E}_k(J, 111)$ and wave functions of states J^π_k for spins $J \leq 27/2$ and parities $\pi = \pm 1$ of the nucleus in question. The results of the calculation are compared with new experimental data for ^{111}Ru presented in ref. [2]. The electromagnetic properties of the nucleus, like spectroscopic electric and magnetic moments and transition probabilities, are calculated as well. However, so far there are no experimental data for those quantities to compare with the calculations. All branching ratios quoted in the paper are calculated with the experimental values of energies and the theoretical reduced matrix elements of the multipole operators.

4.2.1 Positive-parity states

The theoretical (upper part) and experimental (lower part) spectra of positive-parity states are shown in fig. 4. It is seen that the calculations reproduce all levels observed in the experiment. Band 1 has been identified for the first time in nuclei of $A \approx 110$ in ref. [2]. The existence of state $1/2^+_1$ and the band built on it is explained theoretically here. The calculations suggest that state $1/2^+_1$ is the ground state of ^{111}Ru and is placed about 85 keV below the $5/2^+_1$ level. On the other hand, the experiment of ref. [2] points at state $5/2^+_1$, the head of band 3, as being the ground state, whereas the $1/2^+_1$ level is located 10 keV higher. This small difference between the experiment and theory is probably beyond the accuracy of the model predictions. It is worth adding that a recent research [18] shows that the ground state of the neighbouring isotope ^{113}Ru has just spin-parity $1/2^+$.

The positive-parity bands have a complicated internal structure. This is seen in table 1 where the probabilities of the four largest components of the band heads of positive parity are listed. We see that this is especially the case for the lowest-energy and also lowest-spin levels. A dominant contribution to the wave functions of all states of bands 1, 2, 3 and 4 is from the states 0^+_1, 2^+_1, 4^+_1, ... of the ground-state bands of the lighter and heavier cores coupled to the single-particle and single-hole neutron states, respectively. The wave functions of states of higher energy and spin become purer. The model predicts also states built on other core states, *e.g.*, 2^+_2, 3^+_1, 4^+_2, ..., which have not been observed in experiment of ref. [2]. For instance, the calculation gives state $1/2^+_2$ of dominant configuration $2d_{5/2} \otimes 2^+_2$ and energy somewhat higher than 0.5 MeV (cf. upper part of fig. 4). Among the six lowest calculated states of spins $J^\pi \leq 27/2^+$ and energies $\mathcal{E}_k(J) \leq 4.5$ MeV there is no state with an essential contribution from the neutron orbital $1g_{9/2}$ which is involved in the basis of single-neutron states (cf. sect. 4.1.2).

According to the calculations, the states belonging to band 1 show a strong configuration mixing. The dominant components are the $3s_{1/2}$, $2d_{3/2}$, $2d_{5/2}$ and $1g_{7/2}$ single-particle and single-hole neutron states coupled to the yrast states of both cores, correspondingly. Higher-spin states of the band become purer. The dominant single-particle component is then $2d_{5/2}$ with quite a large admixture of $1g_{7/2}$. The calculated branching ratios in band 1 are in a qualitative agreement with the experimental data, as is seen in fig. 4. The most considerable deviations of results of the calculation from the experimental values are observed in the cases of states $9/2^+_3$ and $5/2^+_2$. The former state decays relatively strongly to state $7/2^+_1$ of band 4, what is not observed in the experiment. The latter, according to the calculation, decays to state $3/2^+_1$ of band 2 much weaker than the experiment shows. Configurations similar to those contributing to band 1 enter into the wave functions of the states of band 2. The dominant single-particle configuration at higher spins is again $2d_{5/2}$ but now with admixture of $2d_{3/2}$. The calculations show that the states of this band decay partly to band 3 what is not observed in the experiment. The most substantial difference between the calculation and the observation concerns the decay properties of state $7/2^+_2$ of band 2, which according to the calculation decays strongly to state $5/2^+_1$ of band 3 rather than to state $3/2^+_1$ of band 2, as observed in the experiment. Bands 3 and 4 have a simpler internal structure than that of bands 1 and 2. The single-particle content of the wave functions changes along these bands. The single-neutron components display both, the particle and the hole character. The main configuration of state $5/2^+_1$ of band 3 is $2d_{5/2} \otimes 0^+_1$, whereas the single-neutron orbital

Table 1. The calculated structure of the wave functions of selected positive-parity states of ^{111}Ru. The four largest components are listed for each state. The contributions from the single-particle state coupled to the lighter core $(A-1)$ and the single-hole state coupled to the heavier core $(A+1)$ are given separately for every component. The abbreviation "b.n." stands for "band number".

State J^π_k	b.n.	Component $nl_j \otimes R^+_k$	Probability (%) $A-1$	$A+1$
$1/2^+_1$	1	$3s_{1/2} \otimes 0^+_1$	14	15
		$2d_{3/2} \otimes 2^+_1$	11	18
		$2d_{5/2} \otimes 2^+_1$	10	11
		$1g_{7/2} \otimes 4^+_1$	8	8
$3/2^+_1$	2	$3s_{1/2} \otimes 2^+_1$	8	14
		$2d_{3/2} \otimes 0^+_1$	10	10
		$2d_{3/2} \otimes 2^+_1$	7	9
		$2d_{5/2} \otimes 4^+_1$	7	8
$5/2^+_1$	3	$2d_{5/2} \otimes 2^+_1$	24	17
		$2d_{5/2} \otimes 0^+_1$	16	17
		$1g_{7/2} \otimes 2^+_1$	7	4
		$1g_{7/2} \otimes 4^+_1$	3	1
$7/2^+_1$	4	$1g_{7/2} \otimes 0^+_1$	18	17
		$2d_{5/2} \otimes 2^+_1$	16	12
		$2d_{5/2} \otimes 4^+_1$	9	3
		$1g_{7/2} \otimes 2^+_1$	7	0

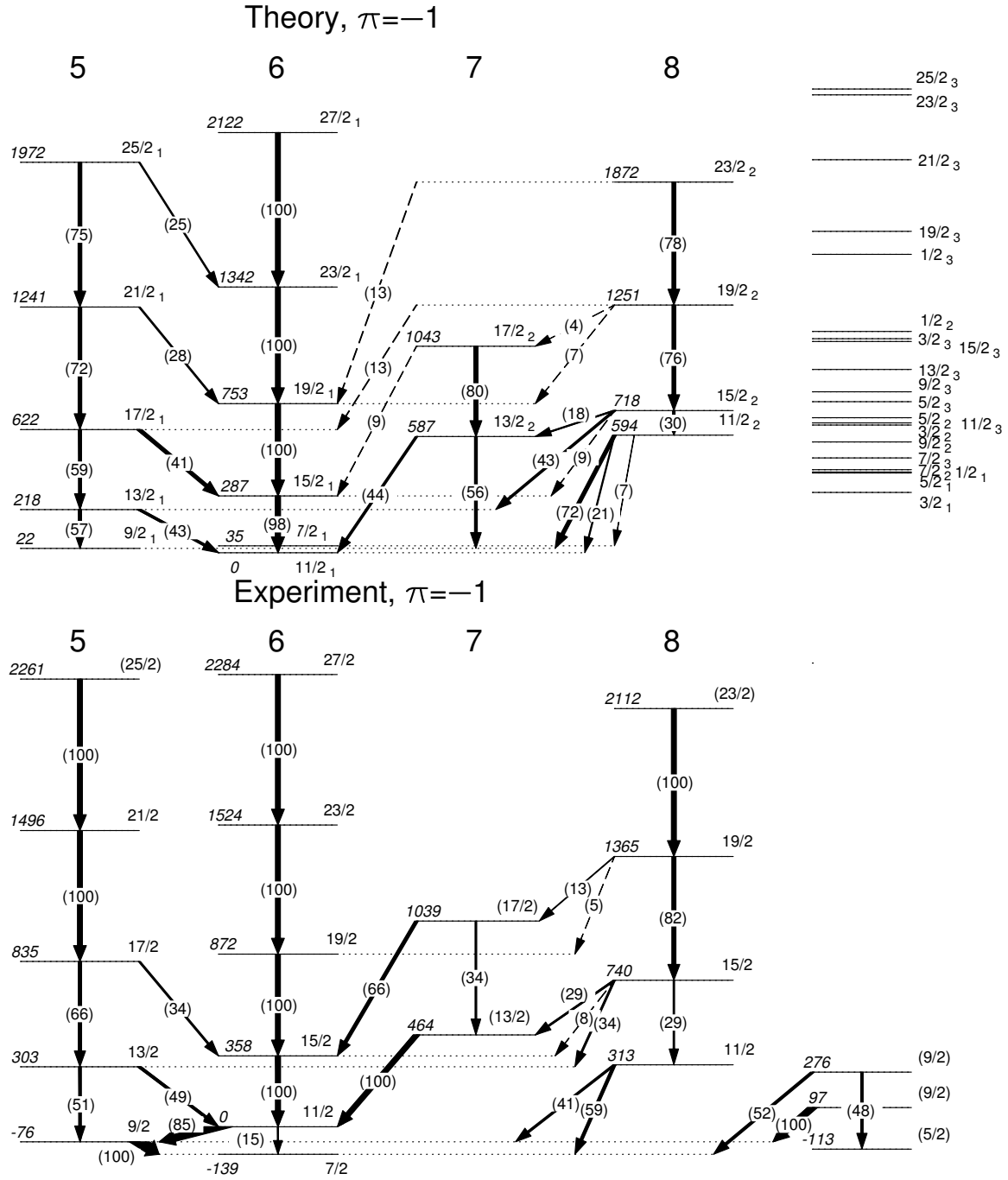

Fig. 5. The same as in fig. 4 but for the negative-parity states. The energy of the $11/2^-_1$ level is put equal to zero.

$1g_{7/2}$ coupled to the yrast core states becomes gradually the main component for higher and higher spins. Similarly, the orbitals $1g_{7/2}$ and $2d_{5/2}$ which are dominant within the state $7/2^+_1$ of band 4 are replaced again by orbital $1g_{7/2}$ at higher-spin states of the band. In general, with the increasing value of spin and energy along the band the states have a purer and purer configuration. For instance, the wave function of state $23/2^+_1$ of band 4 has configurations $1g_{7/2}\otimes 8^+_1$ and $1g_{7/2}\otimes 10^+_1$ in 61% and 12%, respectively. The decay properties of the states in bands 3 and 4 are well reproduced in the calculation.

4.2.2 Negative-parity states

The calculated (top) and experimental (bottom) negative-parity energy levels are shown in fig. 5. Most of the levels observed in the experiment have their theoretical counterparts except for the three states, namely two states

Table 2. The same as in table 1 but for selected negative-parity states.

State J_k^π	b.n.	Component $nl_j \otimes R_k^+$	Probability (%) $A-1$	$A+1$
$9/2_1^-$	5	$1h_{11/2} \otimes 2_1^+$	42	31
		$1h_{11/2} \otimes 6_1^+$	8	2
		$1h_{11/2} \otimes 4_1^+$	0	8
		$2f_{7/2} \otimes 2_1^+$	1	2
$7/2_1^-$	6	$1h_{11/2} \otimes 4_1^+$	28	15
		$1h_{11/2} \otimes 2_1^+$	17	27
		$1h_{11/2} \otimes 6_1^+$	4	0
		$2f_{7/2} \otimes 0_1^+$	1	2
$11/2_1^-$	6	$1h_{11/2} \otimes 0_1^+$	29	31
		$1h_{11/2} \otimes 4_1^+$	12	3
		$1h_{11/2} \otimes 2_1^+$	0	7
		$1h_{11/2} \otimes 6_1^+$	1	5
$13/2_2^-$	7	$1h_{11/2} \otimes 2_2^+$	30	38
		$1h_{11/2} \otimes 6_2^+$	3	3
		$1h_{11/2} \otimes 2_4^+$	2	2
		$1h_{11/2} \otimes 4_2^+$	4	0
$11/2_2^-$	8	$1h_{11/2} \otimes 2_2^+$	17	23
		$1h_{11/2} \otimes 4_1^+$	10	7
		$1h_{11/2} \otimes 5_1^+$	4	2
		$1h_{11/2} \otimes 2_4^+$	2	3

of spin $9/2^-$ and one $5/2^-$ state shown in the rightmost column of the lower part of fig. 5. The spin and parity assignments are only tentative for all these three levels. This is why we do not try to draw conclusions concerning their origin. According to the calculation the lowest negative-parity state is $11/2_1^-$. Two other levels, namely $9/2_1^-$ and $7/2_1^-$, are predicted to be placed slightly above: 22 keV and 35 keV, respectively. Such a narrow multiplet is also observed in the experiment [2] but with a different ordering of the states, namely $7/2_1^-$, $9/2_1^-$ and $11/2_1^-$. The lowest observed negative-parity state $7/2_1^-$ is located 254 keV above the lowest experimental positive-parity state $5/2_1^+$ [2]. The corresponding calculated energy equals 297 keV, quite close to the observed value. The calculated position of the $11/2_2^-$ level belonging to band 8 as well as its decay properties do not agree with the experimental data. From experience of the present calculations we know that increasing the value of strength χ_2 improves results in this respect. It was already mentioned in sect. 2 that a change of χ_2 simulates the corresponding change of the quadrupole deformation. Therefore, a need to change the core-particle interaction strength could be a signature that the odd neutron in state $1h_{11/2}$ polarizes the core in a different way than that in a positive-parity state.

The structure of the negative-parity states is much simpler than that of those of positive-parity discussed in sect. 4.2.1 above. This is understandable since the main neutron orbital contributing to these states is the $1h_{11/2}$ intruder state in the valence neutron shell $50 < N \leq 82$. For instance, the contribution of $2f_{7/2}$ orbital to the $7/2_1^-$ state is only of 5 % according to the calculation. However, we notice that although the calculated contributions to the negative-parity states coming from low-spin neutron orbitals $3p_{1/2}$, $3p_{3/2}$, $2f_{5/2}$ and $2f_{7/2}$ are small, taking these orbitals into account is of importance in the calculation. Indeed, these single-neutron states affect the positions of some low-spin levels of ^{111}Ru. The $9/2_1^-$, $13/2_1^-$, $17/2_1^-$, $21/2_1^-$ and $25/2_1^-$ states of band 5 are predominantly composed of the 2_1^+, 2_1^+, 4_1^+, 6_1^+ and 8_1^+ states, respectively, of the $A = 110$ and $A = 112$ cores. Similarly, the states belonging to band 6 with spins $11/2^-$, $15/2^-$, $19/2^-$, $23/2^-$ and $27/2^-$ are built on the 0_1^+, 2_1^+, 4_1^+, 6_1^+ and 8_1^+ core states, respectively. Bands 7 and 8 are based on the quasi-γ band of both cores. The $13/2_2^-$ and $17/2_2^-$ states of band 7 correspond to the 2_2^+ and 3_1^+ core states, respectively, whereas states $11/2_2^-$, $15/2_2^-$, $19/2_2^-$ and $23/2_2^-$ of band 8 come from the 2_2^+, 2_2^+, 4_2^+ and 6_2^+ core states, respectively. It is interesting that the positive-parity bands containing such quasi-γ core configurations are not observed experimentally, as mentioned already in sect. 4.2.1. Theoretically, such positive-parity bands are located higher than the analogous bands of negative parity. This higher energy perhaps explains why those positive-parity states are populated weakly in the spontaneous fission process which is used as a source of the ^{111}Ru nuclei in the experiment of ref. [2]. The structure of selected negative-parity states is listed in table 2.

Table 3. Calculated magnetic dipole moments, μ and electric quadrupole moments, Q, of selected positive- and negative-parity states of ^{111}Ru.

State J_k^π	b.n.	μ (μ_N)	Q ($e \cdot b$)
$5/2_1^+$	3	−0.46	1.20
$3/2_1^+$	2	0.78	−0.67
$1/2_1^+$	1	0.02	0.
$11/2_1^-$	6	−0.70	−0.29
$9/2_1^-$	5	−0.83	0.23
$7/2_1^-$	6	−1.07	0.97

4.2.3 Electromagnetic properties

There are no experimental data on electromagnetic properties of nucleus ^{111}Ru till now. Here, in table 3 we show as an instance the theoretical predictions for spectroscopic moments of a few of its selected states.

5 Summary and conclusions

The structure of nucleus ^{111}Ru treated as a system of the odd, 67th neutron coupled to the neighbouring even-even cores, ^{110}Ru and ^{112}Ru, has been investigated in the frame of the Core-Quasiparticle Coupling model. According to the model the neutron is a quasiparticle, being a particle

on the top of the lighter core and a hole in the heavier one. The present calculation has confirmed the importance of the pairing interaction involved in the CQPC model: the particle and hole contributions have turned out to be, in general, both essential in the states of the even-odd nucleus in question. It is a matter of course since the neutron Fermi level for $N = 67$ is in the middle of the valence shell. Since the characteristics of both cores are very similar it has been assumed for simplicity that they are the same and correspond to those of ^{110}Ru. The excitation energies and quadrupole matrix elements for ^{110}Ru have been taken from calculations of ref. [7] performed in the frame of collective "quadrupole plus pairing" model. The Bohr Hamiltonian has been determined fully from a microscopic theory without any free parameter. Due to that approach to collective excitations it became feasible to extract properties of collective states from a microscopic theory and obtain results compatible with experimental data with no adjustable parameters. Characteristics of collective states of an even-even nucleus got that way are for the first time used in the present research to describe an odd nucleus within CQPC model. There is only one free parameter in the CQPC calculations for even-odd nuclei. This is the core-particle coupling strength χ_2 for quadrupole-quadrupole interaction. In the case of ^{111}Ru the value $\chi_2 = 15\,\mathrm{MeV}$ has been found to give reasonable results. This value is close to value $\chi_2 \approx 11\,\mathrm{MeV}$ suggested by Arima in ref. [16] but far from the estimation $\chi_2 \approx 40\,\mathrm{MeV}$ by Bès and Sorensen [9]. More data, especially for low-spin states, would be necessary to confirm the present choice of χ_2 for nuclei of $A \approx 110$.

All experimental positive-parity states have been reproduced in the present calculation. This suggests that neither the prolate-oblate shape coexistence nor the normal-extended deformation coexistence occur in states of ^{111}Ru observed experimentally. Should the shape and/or the deformation coexistence exists some additional states would appear which would not be explained in the present calculation. The ^{110}Ru core is a triaxial γ-soft nucleus in the view of the theory of ref. [7] and the collective wave functions can be localized neither around $\gamma = 0$ nor around $\gamma = \pi/3$. Also, the collective potential energy surface for ^{110}Ru does not possess a second minimum, as we have seen in fig. 1. The core polarization effect is, apparently, not strong enough here to change substantially localizations of the wave functions of ^{111}Ru in the deformation space.

A strong configuration mixing of single-neutron states $3s_{1/2}$, $2d_{3/2}$, $2d_{5/2}$ and $1g_{7/2}$ coupled to the yrast states of the cores has been obtained for positive-parity bands in the present calculation. It becomes gradually weaker for higher-energy and higher-spin members of the bands. The dominant single-particle configurations are then $2d_{5/2}$ for bands 1 and 2 with quite a large admixture of $1g_{7/2}$ and $2d_{3/2}$, respectively, and $1g_{7/2}$ for bands 3 and 4. The band built on state $1/2_1^+$, which has for the first time been observed in experiment of ref. [2] for nuclei of $A \approx 110$, is reproduced by the present model.

All four negative-parity bands observed in the experiment have been explained theoretically. These bands have a relatively simple structure according to the present theory. The dominant configuration is the single-neutron $1h_{11/2}$ quasiparticle state coupled to the core ground-state band. There are also predicted negative-parity states corresponding to the $1h_{11/2}$ neutron orbital coupled to the core quasi-γ states 2_2^+, 3_1^+, 4_2^+, ... The states of positive parity built on the quasi-γ core states are predicted to have higher energy than those of negative parity. This explains why such "quasi-γ" states of negative parity are observed in experiment [2] whereas those of positive parity are not. Apparently, the latter ones are hardly populated in the process of spontaneous fission serving as a source of ^{111}Ru in the experiment [2].

To sum up one should point out some characters of the present calculation. The collective properties of the even-even cores, ^{110}Ru and ^{112}Ru, used in the calculation have originated from a microscopic theory and have not been adjusted to data. Only one free parameter has been used in description of coupling the odd neutron to both cores. As the Fermi level is placed in the middle of the valence shell the states of ^{111}Ru possess a complicated quasiparticle structure. All eight positive- and negative-parity bands observed experimentally have been identified and explained in the frame of the CQPC model. In view of all these circumstances the conclusion is that the results are in a remarkable agreement with experimental data.

The present work was supported in part by the Polish Committee for Scientific Research (KBN) under contract no. 2P03B04119.

References

1. J.A. Shannon, W.R. Phillips, J.L. Durell, B.J. Varley, W. Urban, C.J. Pearson, I. Ahmad, L.R. Morss, K.L. Nash, C.W. Williams, N. Schultz, E. Lubkiewicz, M. Bentaleb, Phys. Lett. B **336**, 136 (1994).
2. W. Urban, T. Rząca-Urban, Ch. Droste, S.G. Rohoziński, J.L. Durell, W.R. Phillips, A.G. Smith, B.J. Varley, N. Schultz, I. Ahmad, J.A. Pinston, this issue, p. 231.
3. F. Dönau, S. Frauendorf, Phys. Lett. B **71**, 263 (1977).
4. F. Dönau, U. Hagemann, Z. Phys. A **293**, 31 (1979).
5. Ch. Droste, D. Chlebowska, J. Dobaczewski, F. Dönau, A. Kerek, G. Leander, J. Srebrny, W. Waluś, Nucl. Phys. A **341**, 98 (1980).
6. D. Troltenier, J.P. Draayer, B.R.S. Babu, J.H. Hamilton, A.V. Ramayya, V.E. Oberacker, Nucl. Phys. A **601**, 56 (1996).
7. K. Zając, L. Próchniak, K. Pomorski, S.G. Rohoziński, J. Srebrny, Nucl. Phys. A **653**, 71 (1999).
8. S.G. Rohoziński, K. Pomorski, L. Próchniak, K. Zając, Ch. Droste, J. Srebrny, Yad. Fizika **64**, 1081 (2001).
9. D.R. Bès, R.A. Sorensen, in *Advances in Nuclear Physics*, edited by M. Baranger, E. Vogt, Vol. **2** (Plenum Press, New York, 1969) p. 129.
10. A. Kerman, A. Klein, Phys. Rev. **132**, 1326 (1963).
11. P. Protopapas, A. Klein, N.R. Walet, Phys. Rev. C **50**, 245 (1994).

12. S. Raman, C.H. Malarkey, W.T. Milner, C.W. Nestor jr., P.H. Stelson, At. Data Nucl. Data Tables **36**, 1 (1987).
13. D. DeFrenne, E. Jacobs, Nucl. Data Sheets **89**, 481 (2000).
14. T. Seo, Z. Phys. **43**, 324 (1986).
15. A. Bohr, B.R. Mottelson, *Nuclear Structure*, Vol. **I** (New York, Amsterdam, 1969) figs. 2-30, p. 239.
16. A. Arima, Nucl. Phys. A **354**, 19c (1981).
17. K. Starosta, C.J. Chiara, D.B. Fossan, T. Koike, D.R. LaFosse, G.J. Lane, J.M. Sears, J.F. Smith, A.J. Boston, P.J. Nolan, E.S. Paul, A.T. Semple, M. Devlin, D.G. Sarantites, I.Y. Lee, A.O. Macchiavelli, Phys. Rev. C **61**, 034308 (2000).
18. J. Kurpeta, private communication.